MECSOL 2019 - Proceedings of the 7th International Symposium on Solid Mechanics,
V. Tita, A. Ferreira, M.L. Ribeiro, A. Vieira and A.T. Beck (Editors), ABCM, Sao Carlos, SP, Brazil, April 15th to 17th, 2019

Evaluation of the Souza–Auricchio Shape Memory Alloy Model using Axial-Torsional Test Data

T. F. Fonseca, F. C. Castro

Department of Mechanical Engineering, University of Brasília, 70910-900 Brasília, DF, Brazil

Abstract: There is an increasing need for three-dimensional shape memory alloy (SMA) constitutive models that can predict stress and strain states with a reasonable accuracy for a wide range of multiaxial loading conditions. Despite of that, experimental evaluations of SMA models have been limited to restricted loading conditions. In this work, the Souza–Auricchio model is evaluated using axial-torsional test data available in the literature to identify its limitations. Numerical simulations of the stress-strain hysteresis loop of thin-walled tubes subjected to axial-torsional loading indicated that the Souza–Auricchio model cannot describe the shear behavior with acceptable accuracy.

Keywords: shape memory alloys, Souza–Auricchio model, experimental evaluation, axial-torsional

INTRODUCTION

Shape memory alloys (SMAs) constitute a class of metallic alloys with characteristic mechanical and thermomechanical properties, known as pseudoelasticity and shape memory effect. Due to these properties, SMAs have become popular in applications involving sensors, actuators, and shock dampers. In addition, the increasing demand for intelligent materials (i.e., materials capable of responding to external stimuli in a functional way) has boosted research on the microstructural mechanisms, properties and applications of SMAs.

In the last three decades, many SMA constitutive models have been proposed. Among them, the model developed by Souza, Mamiya & Zouain (1998) and improved by Auricchio & Petrini (2004) provides a suitable framework for the three-dimensional stress-strain analysis of engineering components. The Souza–Auricchio model presents a simple and robust solution algorithm, which is fundamental for its implementation within finite element codes. Since 2012, this model is available in the commercial finite element package ANSYS®.

Although a wide range of axial-torsional test data for SMA materials have been reported (Tab. 1), experimental evaluations of the Souza–Auricchio model have been limited to restricted loading conditions. In this work, the stress-strain behavior described by the Souza–Auricchio model is evaluated, from both a qualitative and a quantitative perspective, using extensive axial-torsional test data.

Table 1 – Experimental data of SMAs under axial-torsional loading.

Reference	Material	Specimen	Control Mode
Sittner, Hara & Tokuda (1995)	Cu-Al-Zn-Mn	Thin-walled Tube	Force, Displacement
Sittner et al. (1996)	Cu-Al-Zn-Mn	Thin-walled Tube	Force, Displacement
Rogueda, Lexcellent & Bocher (1996)	Cu-Zn-Al	Thin-walled Tube	Force
Tokuda et al. (1999)	Cu-Al-Zn-Mn	Thin-walled Tube	Force, Temperature
Thamburaja & Anand (2002)	Ni-Ti	Thin-walled Tube	Displacement
Tokuda et al. (2002)	Cu-Al-Zn-Mn	Thin-walled Tube	Force, Temperature
McNaney et al. (2003)	Ni-Ti	Thin-walled Tube	Displacement
Wang, Yue & Wang (2007)	Ni-Ti	Thin-walled Tube	Displacement
Grabe & Bruhns (2008)	Ni-Ti	Solid Cylinder	Displacement
Sittner et al. (2009)	Ni-Ti	Thin Wire	Displacement, Temperature
Wang et al. (2010)	Ni-Ti	Thin-walled Tube	Displacement
Mehrabi et al. (2014)	Ni-Ti	Thin-walled Tube	Displacement
Mehrabi et al. (2015)	Ni-Ti	Thin-walled Tube	Force, Displacement

SOUZA–AURICCHIO SMA MODEL

The Souza–Auricchio model (Souza, Mamiya & Zouain, 1998; Auricchio & Petrini, 2004) is based on a free energy density function Ψ defined as

$$\Psi(\theta, \boldsymbol{e}, \boldsymbol{e}^{tr}, T) = \frac{1}{2}K\theta^2 + G\left\|\boldsymbol{e} - \boldsymbol{e}^{tr}\right\|^2 + \beta(T - T^*)^+\left\|\boldsymbol{e}^{tr}\right\| + \frac{1}{2}h\left\|\boldsymbol{e}^{tr}\right\|^2 + I_{\varepsilon L}(\boldsymbol{e}^{tr}), \tag{1}$$

where θ and $\boldsymbol{e}$ are, respectively, the volumetric and the deviatoric part of the total strain $\boldsymbol{\varepsilon}$, while $\boldsymbol{e}^{tr}$ is the transformation strain. K and G are the bulk and the shear moduli, respectively. β is temperature scaling parameter, T^* is the martensitic finish temperature, and h is a material hardening parameter. $I(\boldsymbol{e}^{tr})$ is an indicator function introduced to satisfy the constraint on the transformation strain norm, defined as

$$I_{\varepsilon L}(\boldsymbol{e}^{tr}) = \begin{cases} 0, & \text{if } \left\|\boldsymbol{e}^{tr}\right\| \le \varepsilon_L, \\ +\infty, & \text{otherwise.} \end{cases} \tag{2}$$

where ε_L is the maximum transformation strain. Following standard arguments, the thermodynamic forces are expressed as follows

$$\begin{cases} p = \dfrac{\partial \psi}{\partial \theta} = K\theta, \\ \boldsymbol{s} = \dfrac{\partial \psi}{\partial \boldsymbol{e}} = 2G(\boldsymbol{e} - \boldsymbol{e}^{tr}), \\ \boldsymbol{X} = -\dfrac{\partial \psi}{\partial \boldsymbol{e}^{tr}} = \boldsymbol{s} - \beta(T - T^*)^+ \dfrac{\boldsymbol{e}^{tr}}{\left\|\boldsymbol{e}^{tr}\right\|} - h\boldsymbol{e}^{tr} - \gamma \dfrac{\boldsymbol{e}^{tr}}{\left\|\boldsymbol{e}^{tr}\right\|}, \end{cases} \tag{3}$$

where p and $\boldsymbol{s}$ are, respectively, the volumetric and the deviatoric part of the stress $\boldsymbol{\sigma}$, while $\boldsymbol{X}$ is a thermodynamic stress-like quantity associated to the transformation strain $\boldsymbol{e}^{tr}$. The γ variable arises from the differentiation of the indicator function $\partial I_{\varepsilon L}(\boldsymbol{e}^{tr})$ and is defined as

$$\begin{cases} \gamma = 0, & \text{if } \left\|\boldsymbol{e}^{tr}\right\| < \varepsilon_L, \\ \gamma \ge 0, & \text{if } \left\|\boldsymbol{e}^{tr}\right\| = \varepsilon_L, \end{cases} \tag{4}$$

so that $\partial I_{\varepsilon L}(\boldsymbol{e}^{tr}) = \gamma \dfrac{\boldsymbol{e}^{tr}}{\left\|\boldsymbol{e}^{tr}\right\|}$.

To control the evolution of the internal variable ε^{tr}, a limit function F is introduced

$$F(\boldsymbol{X}) = \left\|\boldsymbol{X}\right\| - R, \tag{5}$$

where R is the radius of the elastic domain. The evolution equation of the variable $\boldsymbol{e}^{tr}$ is given by

$$\dot{\boldsymbol{e}}^{tr} = \dot{\zeta}\frac{\partial F}{\partial \boldsymbol{X}} = \dot{\zeta}\frac{\boldsymbol{X}}{\left\|\boldsymbol{X}\right\|}. \tag{6}$$

Also, in order to satisfy the principle of maximum dissipation for the evolution of internal variables, the Kuhn-Tucker conditions must be satisfied:

$$\dot{\zeta} \ge 0, \qquad F \le 0, \qquad \dot{\zeta} F = 0, \tag{7}$$

with $\dot{\zeta}$ being the evolution of the volumetric fraction in the phase transformation.

DETERMINATION OF MATERIAL CONSTANTS

The Souza–Auricchio model requires the determination of eight material constants (E_A, E_M, R, ε_L, β, T^*, h, and m). Often these constants are determined based on a mechanical loading-unloading test and a thermal cycling test with constant axial tension.

Figure 1a illustrates the constants that can be determined from a stress-strain hysteresis loop: Young's modulus of austenite (E_A), Young's modulus of martensite (E_M), the radius of the elastic domain (R), the maximum transformation strain (ε_L), and the hardening parameter (h). From the strain versus temperature diagram obtained from the thermal cycling test (Fig. 1b), the temperature scaling parameter (β) can be determined and the martensitic finish temperature (T^*) can be calculated using Eq. (8). In this work, the Lode parameter (m) is set equal to zero, which means that the SMA behavior is symmetric under tension and compression.

$$T^* = T_{yM} + \frac{(R-\sigma)}{\beta}. \tag{8}$$

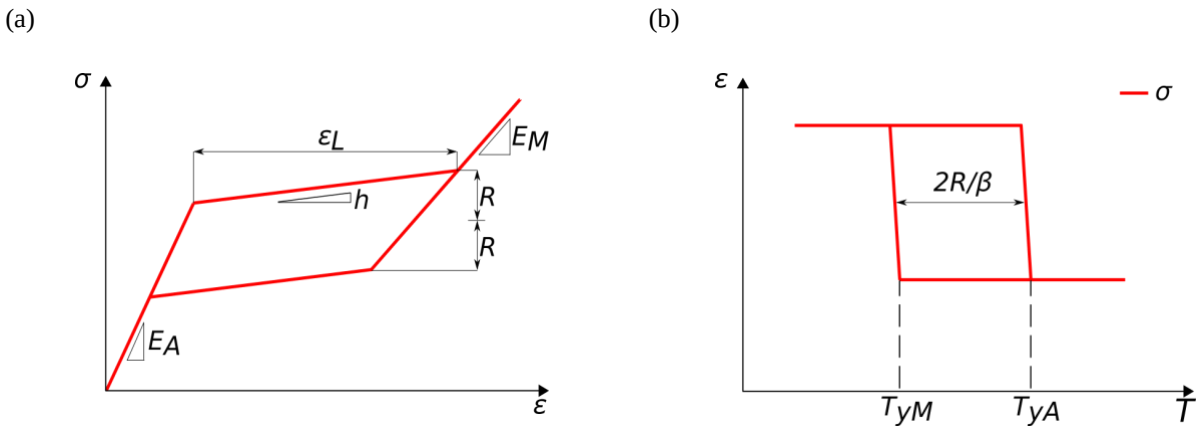

Figure 1 – Constants of the Souza–Auricchio model related to (a) stress-strain hysteresis loop and (b) strain versus temperature diagram.

EXPERIMENTAL EVALUATION

Numerical simulations were performed using the commercial finite element package ANSYS®. The specimens were discretized using the beam element type BEAM 188. This element was chosen not only because of its capability to account for large rotations/strains, but also because it is suitable for analyzing slender structures.

Test data from Sittner et al. (2009)

Figures 2 and 3 show the simulation results for some of the tests performed by Sittner et al. (2009). These tests were conducted with a constant tensile stress and by applying a fully reversed angular displacement. All the experiments were carried out on NiTi wires with a diameter of 0.1 mm. A Peltier furnace was used to control the temperature of the samples during the experiments. The results indicate that the Souza–Auricchio model can provide a qualitative description of the observed behavior, even at different temperatures. However, the predicted torque and axial strain are not accurate.

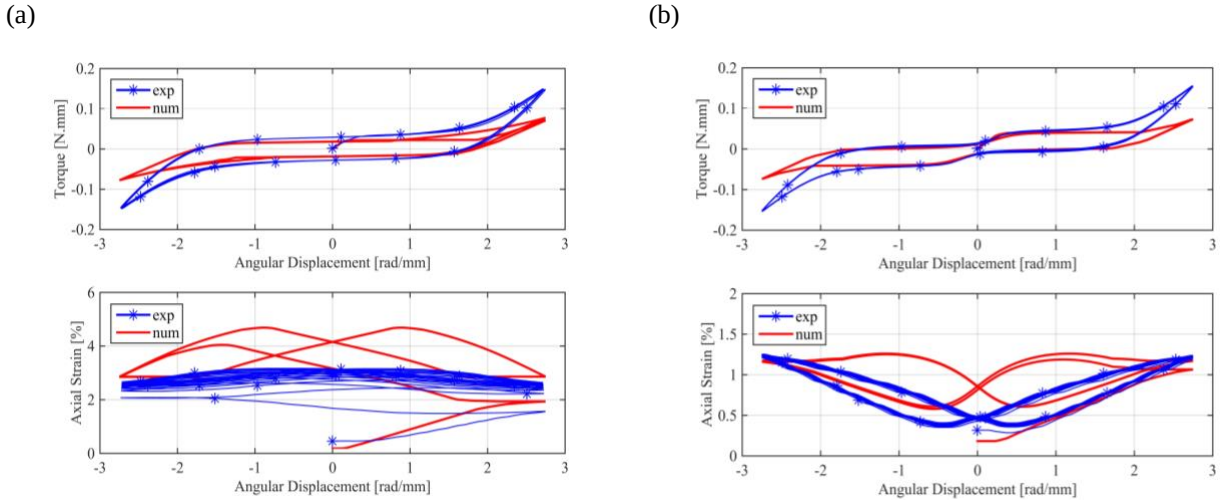

Figure 2 – Torque vs angular displacement and axial strain vs angular displacement curves at 70 MPa. Temperature equals to (a) -30 °C and (b) -10 °C.

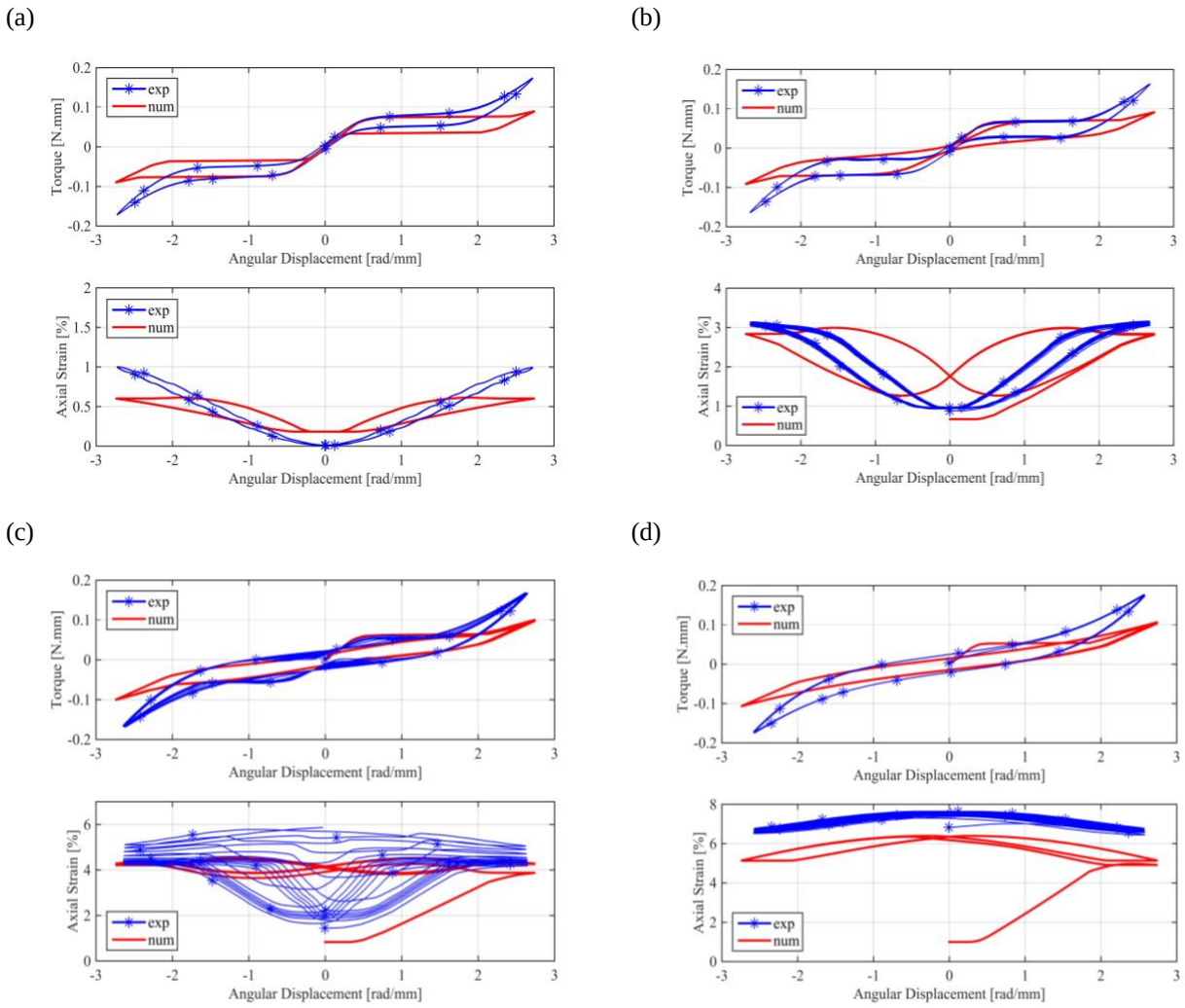

Figure 3 – Torque vs angular displacement and axial strain vs angular displacement curves at 30 °C. Axial tension equals to (a) 70 MPa, (b) 255 MPa, (c) 317 MPa, and (d) 379 MPa.

Test data from Wang et al. (2010)

In the work of Wang et al. (2010), cyclic proportional and non-proportional tension-torsion experiments were performed on NiTi thin-walled tubes. Axial displacement and torsional angle were chosen as the control parameters. Three types of sinusoidal strain paths were selected for the experiments: proportional loading, 45°-out-of-phase non-proportional loading and 90°-out-of-phase non-proportional loading. All tests were carried out at room temperature of around 22°C. It is important to remark that the specimens were not trained prior to the experiments, resulting in a transient mechanical response. The experimental and numerical results are compared in Fig. 4.

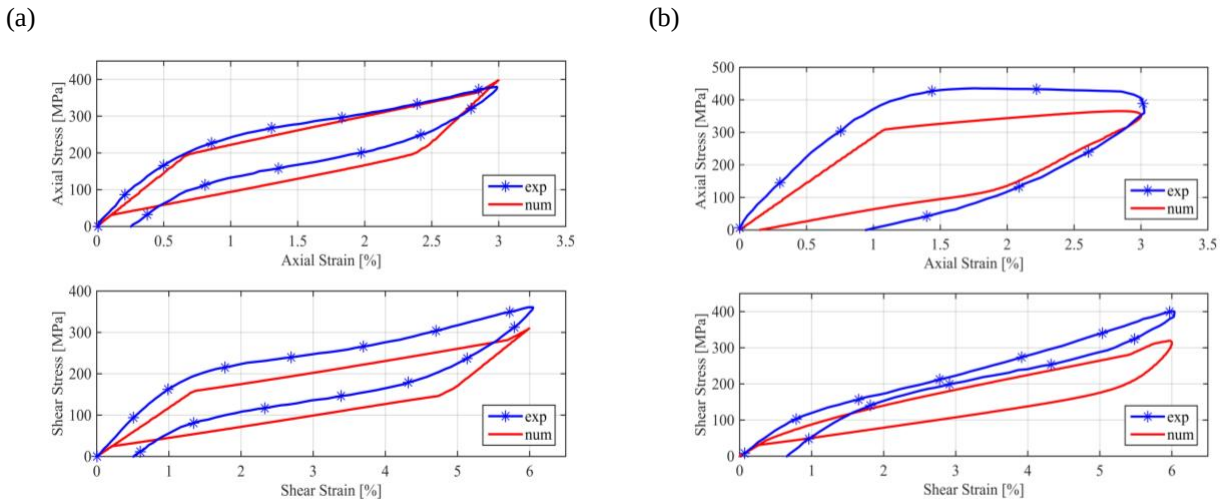

(c)

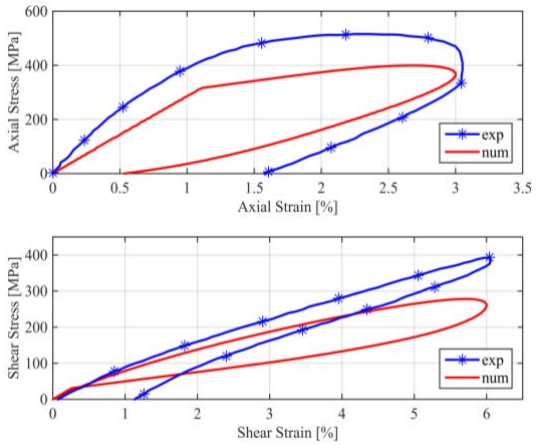

Figure 4 – Axial stress vs axial strain and shear stress vs shear strain curves under (a) proportional loading, (b) 45°-out-of-phase non-proportional loading, and (c) 90°-out-of-phase non-proportional loading.

The performed simulations reveal that the accuracy of the Souza–Auricchio model is closely related to the strain path applied. For example, in the proportional loading case, the difference between the predicted and the observed maximum axial stress is approximately 5% whereas, in non-proportional loading cases, this difference is about 20%.

Note that the shear stress-strain behavior is underestimated in all loading cases. On average, the shear stresses predicted by the model were 21% lower than those observed experimentally. This drawback was already identified in the work of Souza, Mamiya & Zouain (1998) who proposed a slight modification in the original model. The modified model is obtained by substituting the function $F(\boldsymbol{X}) = \|\boldsymbol{X}\| - R$, introduced in Eq. (5), by

$$F(\boldsymbol{X}) = \|\boldsymbol{X}\| + \alpha|y| - R, \tag{9}$$

where y is a thermodynamic force, and α denotes an additional material parameter to be determined by fitting the hysteresis loops in the traction and shear tests. A small improvement was observed after applying the modification.

Test data from Mehrabi et al. (2015)

In the work of Mehrabi et al. (2015), the behaviors of NiTi thin-walled tubes in proportional and non-proportional tension-torsion experiments, on both strain-controlled mode and stress-controlled mode, were investigated. In strain-controlled tests, axial displacement and rotation were chosen as the control parameters. In stress-controlled tests, force and torque were chosen to be the leading parameters. All the experiments were performed at the temperature of 23 °C. Comparisons between the stress-strain hysteresis loops obtained from the proportional tension-torsion tests and the simulations using the Souza–Auricchio model are presented in Fig. 5. In addition, Fig. 6 presents the results obtained from the rectangular non-proportional tension-torsion tests.

(a) (b)

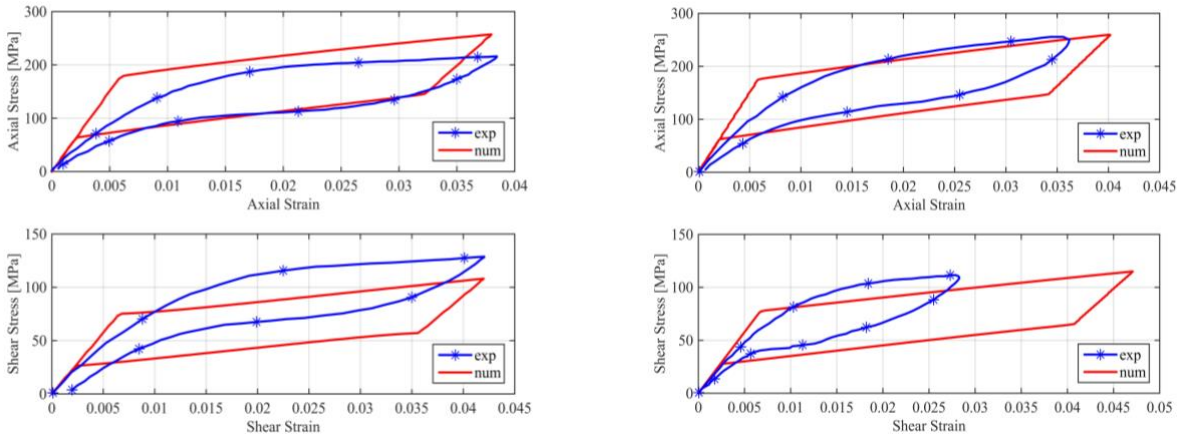

Figure 5 – Observed and simulated stress-strain hysteresis loops under proportional axial-torsional loading: (a) strain-controlled test and (b) stress-controlled test.

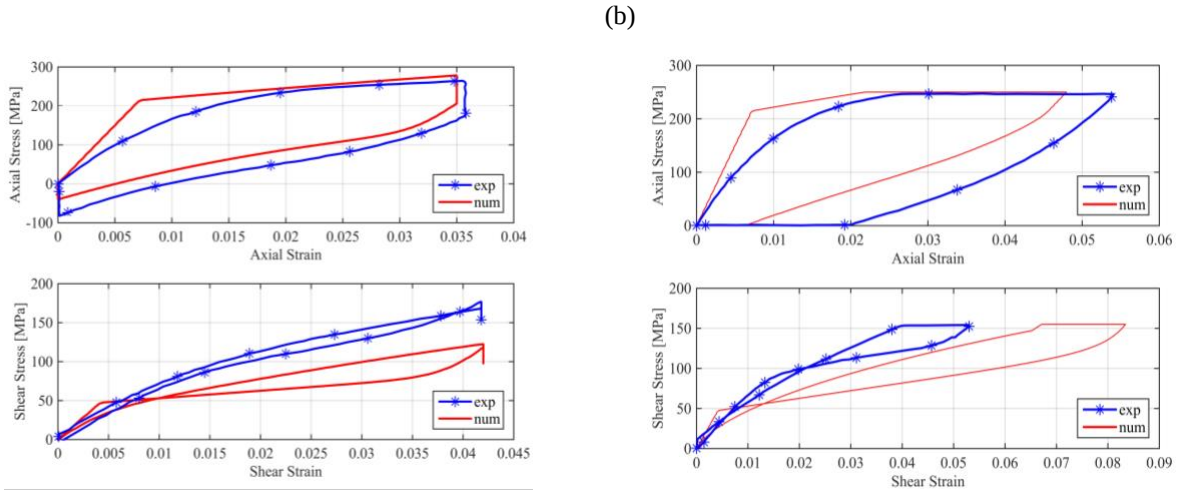

Figure 6 – Observed and simulated stress-strain hysteresis loops under non-proportional axial-torsional loading: (a) strain-controlled test and (b) stress-controlled test.

The axial stress-strain hysteresis loops are reasonably described by the model. However, the simulated shear stress-strain curves are not accurate. For example, in the strain-controlled tests, the simulated shear stresses were up to 30% lower than those observed experimentally whereas, in the stress-controlled tests, the simulated shear strains were approximately 60% higher than those observed. According to Auricchio, Morganti & Reali (2009), the inaccuracy of the Souza–Auricchio model in describing the shear stress-strain behavior could be related to the adopted J2-type yield surface.

CONCLUDING REMARKS

The results obtained in this work for SMA materials under axial-torsional loadings indicated that the Souza–Auricchio model is able to reproduce, from a qualitative point of view, the main characteristics of the stress-strain hysteresis loops. However, the quantitative agreement with experimental data is not good, especially when predicting the shear behavior. Further investigation is still required to know if this inaccuracy also occurs for SMA test data under different axial-torsional loading conditions.

ACKNOWLEDGEMENTS

Tiago Fonseca acknowledges the support from CAPES. Fábio Castro is grateful for the support provided by CNPq (contract 308126/2016-5).

REFERENCES

Auricchio, F., & Petrini, L. (2004). A three-dimensional model describing stress-temperature induced solid phase transformations: solution algorithm and boundary value problems. International Journal for Numerical Methods in Engineering, 61(6), 807-836.

Auricchio, F., Morganti, S., & Reali, A. (2009). SMA numerical modeling versus experimental results. In ESOMAT 2009-8th European Symposium on Martensitic Transformations (p. 08004). EDP Sciences.

Grabe, C., & Bruhns, O. T. (2008). Tension/torsion tests of pseudoelastic, polycrystalline NiTi shape memory alloys under temperature control. Materials Science and Engineering: A, 481, 109-113.

McNANEY, J. M., Imbeni, V., Jung, Y., Papadopoulos, P., & Ritchie, R. O. (2003). An experimental study of the superelastic effect in a shape-memory Nitinol alloy under biaxial loading. Mechanics of Materials, 35(10), 969-986.

Mehrabi, R., Andani, M. T., Elahinia, M., & Kadkhodaei, M. (2014). Anisotropic behavior of superelastic NiTi shape memory alloys; an experimental investigation and constitutive modeling. Mechanics of Materials, 77, 110-124.

Mehrabi, R., Andani, M. T., Kadkhodaei, M., & Elahinia, M. (2015). Experimental study of NiTi thin-walled tubes under uniaxial tension, torsion, proportional and non-proportional loadings. Experimental Mechanics, 55(6), 1151-1164.

Rogueda, C., Lexcellent, C., & Bocher, L. (1996). Experimental study of pseudoelastic behaviour of a Cu Zn AI polycrystalline shape memory alloy under tension-torsion proportional and non-proportional loading tests. Archives of Mechanics, 48(6), 1025-1047.

Sittner, P., Hara, Y., & Tokuda, M. (1995). Experimental study on the thermoelastic martensitic transformation in shape memory alloy polycrystal induced by combined external forces. Metallurgical and Materials Transactions A, 26(11), 2923-2935.

Sittner, P., Heller, L., Pilch, J., Sedlak, P., Frost, M., Chemisky, Y., ... & Auricchio, F. (2009). Roundrobin SMA modeling. In ESOMAT 2009-8th European Symposium on Martensitic Transformations (p. 08001). EDP Sciences.

Sittner, P., Takakura, M., Hara, Y., & Tokuda, M. (1996). On transformation pathways of general stress controlled thermoelastic martensitic transformation in shape memory alloys. Le Journal de Physique IV, 6(C1), C1-357.

Souza, A. C., Mamiya, E. N., & Zouain, N. (1998). Three-dimensional model for solids undergoing stress-induced phase transformations. European Journal of Mechanics-A/Solids, 17(5), 789-806.

Thamburaja, P., & Anand, L. (2002). Superelastic behavior in tension–torsion of an initially-textured Ti–Ni shape-memory alloy. International Journal of Plasticity, 18(11), 1607-1617.

Tokuda, M. T. M. S. P., Ye, M., Takakura, M., & Sittner, P. (1999). Thermomechanical behavior of shape memory alloy under complex loading conditions. International journal of Plasticity, 15(2), 223-239.

Tokuda, M., Sittner, P., Takakura, M., & Haze, M. (2002). Multi-Axial Constitutive Equations of Polycrystalline Shape Memory Alloy. JSME International Journal Series A Solid Mechanics and Material Engineering, 45(2), 276-281.

Wang, X. M., Wang, Y. F., Lu, Z. Z., Deng, C. H., & Yue, Z. F. (2010). An experimental study of the superelastic behavior in NiTi shape memory alloys under biaxial proportional and non-proportional cyclic loadings. Mechanics of Materials, 42(3), 365-373.

Wang, Y. F., Yue, Z. F., & Wang, J. (2007). Experimental and numerical study of the superelastic behaviour on NiTi thin-walled tube under biaxial loading. Computational Materials Science, 40(2), 246-254.

RESPONSIBILITY NOTICE

The authors are the only responsible for the printed material included in this paper.